

Fast Ultrasound Assisted Synthesis of Cu-SAPO-34 for SCR Application

M. Cortés-Reyes, M.C. Herrera, M.A. Larrubia, L.J. Alemany

Dpto. Ingeniería Química, Facultad de Ciencias, Campus de Teatinos, Universidad de Málaga, Málaga, E-29071, Spain

ABSTRACT: A method to synthesize SAPO-34 and incorporate metals in its structure during the preparation was established. Cu-SAPO-34 was synthesized in one step using the hydrothermal method assisted by ultrasound reducing the time in the autoclave up to 4 hours. SAPO-34 shows a chabazite-like structure with a bimodal porous distribution that are maintained with the 2wt% copper incorporation. The incorporation of copper as Cu²⁺ species inside the structure was achieved. Brønsted acid sites were the predominant NH₃ adsorbed species, and the high ammonia retention capacity makes it an effective NH₃-trap. Copper enhances the overall acidity due to the increase of Lewis acid sites. Cu-SAPO-34 was tested for SCR application, and it is very efficient in SCR process in dry conditions with complete nitrogen selectivity in the whole SCR operation temperature window. Nitrates and Cu²⁺(NO) species were detected by FTIR NO adsorption. Mononitrosyl Cu (II) is most likely the active species in the SCR mechanism.

KEYWORDS: One-pot synthesis, Ultrasound assisted, SAPO-34, SCR.

I. INTRODUCTION

An advantage of biodiesel is its potential to significantly reduce most regulated exhaust emissions, with the exception of nitrogen oxides [1,2]. This negative effect is dependent on FAME: petrodiesel blends and the chain-length and double-bonds content of fuels. In order to reduce this impact of NO_x emissions in the transport sector that incorporates diesel engines it becomes more necessary to incorporate the most efficient coupled after-treatment technologies. There are two well-studied technologies for the reduction of these contaminants, such as NSR (NO_x Storage and reduction) and SCR (Selective Catalytic Reduction) [3,4]. The first one works in cyclic conditions where adsorption-desorption periods alternate, producing nitrogen and water and regenerating the catalyst surface [5]. On the other hand, the second technology consists of the use of ammonia from an external reducing agent, e.g. urea, which reacts with NO_x producing N₂ and H₂O, and it is well-established in heavy duty vehicles where it is possible to situate a urea solution tank [6]. In recent times, the coupling of these two technologies is being studied as a promising solution. NSR technology is not enough to achieve zero emissions at the outlet of diesel engines vehicles, due to the formation of a NH₃ slip that is strongly dependent on the formulation and the conditions and could be used by a SCR catalytic bed placed downstream [7,8].

In several studies it is possible to find a lot of materials widely described for their use as SCR catalysts, from vanadia-based systems to zeolites. Nowadays, zeolitic materials are presented as more suitable NH₃-traps due to their acidity and structure [9]. Lots of zeolites have been proposed, such as ZSM5 or BETA, which despite their excellent properties, have water stability problems.

Recently, zeolites with small pore diameter such as chabazite (3.8 Å) have been proposed to improve hydrothermal stability with regard to large pore zeolites [10,11]. Significant numbers of recent works compare this type of structure with other materials and ensure that SAPO-34 acts effectively in the SCR temperature range and resists thermal aging and hydrostability better than others, such as SSZ13, for example [12,13]. Due to this, the search for SAPO-34 microporous materials to be used as a SCR bed is proved. However, there are some studies indicating that the SCR-DeNO_x process suffers from strong diffusional limitations of ammonia and NO_x in the gas and within the solid as catalyst. So that, it was proposed a bimodal pore structure incorporating meso and macro pores in a monolithic structure for denoxing for stationary applications [14].

International Journal of Innovative Research in Science, Engineering and Technology

(An ISO 3297: 2007 Certified Organization)

Vol. 5, Issue 4, April 2016

Zeolites have to include a metal for having redox capacity, iron and copper being the most studied. *M. Colombo et al.*[15] reported that copper-zeolites show a higher storage capacity of NH_3 and nitrates, and present greater activity in the ammonia oxidation. Moreover, it is less sensitive to the feed ratio between NO and NO_2 and increases the effective range of the SCR process to lower temperatures.

Traditionally, these materials have been synthesized by hydrothermal processes and metal-containing molecular sieves have been obtained by post-synthesis ion exchange procedures, such as wet ion exchange or chemical vapor deposition [16], that not ensure a well metal distribution inside the structure. Nevertheless, actual studies are focused on the direct synthesis in one step of these materials, allowing the location of extra-framework copper species in the chabazite cages [10,17].

Hence, this work shows a method, faster than the conventional ones, for the one-pot synthesis of a zeolitic material with chabazite-like structure, incorporating copper inside with a bimodal porous distribution, effective in its applications in the SCR process.

II. EXPERIMENTAL

2.1. Catalyst synthesis

A SAPO-34 material (denoted as SAPO-34h) was synthesized by hydrothermal method, using this molar gel composition: 2 DEA: 0.6 SiO_2 :1 Al_2O_3 :0.2 P_2O_5 :50 H_2O , keeping the mixture autoclaved at 200 °C during 72h. The solid product was filtered and washed with distilled water, and dried overnight at 110 °C. Finally, it was calcined at 550 °C in air for 5h to remove the organic template molecules. In this study, the sources of Al, P and Si were Aluminum isopropoxide 98% (Alfa Aesar), Phosphoric acid 85% (Panreac) and Ludox HS-40 colloidal silica (Aldrich), respectively. The gel preparation was carried out in the following way: firstly, an aluminum suspension was prepared by adding isopropoxide to water (75 wt%), then, water and phosphoric acid were added and vigorously stirred for 2 hours, after that, silica was mixed for 4 hours and finally, the structure-directing agent (DEA, diethylamine) and 5wt% of seeds were added.

To improve the synthesis process, SAPO-34 (denoted as SAPO-34s) was obtained by sonochemical method using the same precursor gel, mentioned above. The equipment used consisted of Ultrasonic Processor UIP1000hd (Hielscher) with unchangeable frequency of 20 kHz using a titanium sonotrode. The ultrasonic power intensity was $300\text{W}\cdot\text{cm}^{-2}$. In this case, the time in the autoclave was reduced up to 4 hours, while the protocol was identical to the used for the SAPO-34h.

Copper was introduced during the synthesis process with a metal loading of 2 wt% (expressed as copper metal). For this purpose, the Cu-complex was prepared by mixing a 20 wt% aqueous solution of copper (II) sulfate 98 wt% (Alfa) with the tetraethylenepentamine 99% (TEPA, Aldrich) and it was stirred for 2h until dissolution was complete. The molar ratio Cu/TEPA was 1:2 and the relation between the complex and the material defined as Cu-TEPA/(Al+P) was 0.081. The complex was added to the precursor gel together with the phosphoric acid.

To compare morphology, structure and reactivity, a commercial SAPO-34 supplied by Albemarle Corporation was used, and was denoted as SAPO-34c.

2.2. Catalyst characterization

X-ray Powder Diffraction data have been recorded with an X'Pert MPD PRO diffractometer (PANalytical) using $\text{Cu K}\alpha_1$ radiation ($\lambda = 1.54059 \text{ \AA}$) and a Ge(1 1 1) primary monochromator. The X-ray tube worked at 45 kV and 35 mA. The measurements were done from 5° to 80° (2θ). The composition of the catalysts was studied by X-ray fluorescence (XRF) with the XGT-5000WR equipment.

N_2 adsorption-desorption isotherms were obtained at 77K using a Micromeritics ASAP 2020 Analyzer. Before the analysis, the samples were outgassed in vacuum ($1\cdot 10^{-3}$ Pa) for 5h at 453K.

SEM micrographs were obtained with the Scanning Electron Microscope JEOL JSM-840. Prior to recording the images, a fine gold layer was sprayed on the samples. TEM images were taken with a Philips CM 200 of 200 kV and TalosTM F200X from FEI was used for the EDX mapping.

UV-Vis Diffuse Reflectance spectra were recorded by using T92+UV Spectrophotometer from PG Instruments, equipped with conventional integrating sphere.

International Journal of Innovative Research in Science, Engineering and Technology

(An ISO 3297: 2007 Certified Organization)

Vol. 5, Issue 4, April 2016

2.3. FTIR Study

FTIR spectra of self-supporting catalyst disks were recorded by a Nicolet Nexus 6700 spectrometer (100 scans, 4 cm^{-1} resolution). Pure powders were pressed into thin wafers ($\approx 20\text{ mg}$) and were activated in the IR cell connected with a conventional outgassing/gas- manipulation apparatus at $500\text{ }^\circ\text{C}$ under vacuum (10^{-3} torr). After the evacuation process, the samples were saturated for 10 min with 10 torr of NH_3 or NO at room temperature. Consecutively, the gas was evacuated from the cell and surface spectra were recorded from room temperature up to $500\text{ }^\circ\text{C}$.

Co-adsorption of probe molecules at different temperatures was carried out in the same equipment. Ammonia was firstly adsorbed and, after evacuation, $\text{NO} + \text{O}_2$ (1:4) were introduced. Simultaneous gas phase and surface spectra were recorded along the time and the gas composition was analyzed by mass spectrometry.

2.4. Catalytic activity

Standard SCR experiments were carried out in a quartz tube reactor connected to the QMS 200 Mass Spectrometer (Pfeiffer Vacuum PrismaTM). The total gas flow was $100\text{ cm}^3\cdot\text{min}^{-1}$ using 60 mg of powder catalyst ($\text{GHSV} = 10^5\text{ h}^{-1}$). The gas flow consisting of 750ppm NH_3 , 750ppm NO and 3% O_2 was fed at different temperatures. Before the experiments, catalysts were conditioned in the same reaction atmosphere.

III. RESULTS AND DISCUSSION

In Fig. 1, the XRD patterns of all the samples are shown. All materials exhibited the typical diffraction patterns of the chabazite structure (JCPDS 01-087-1527) indicated by diffraction peaks at $2\theta = 9.4, 12.9, 16.15, 20.5, 26.1$ and 30.5° characteristic of SAPO-34 samples.

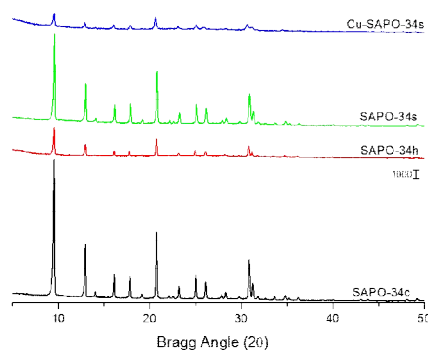


Fig. 1 X-ray diffraction patterns of Cu-free and Cu-containing SAPO catalysts

SAPO-34h showed crystallinity similar to the obtained for SAPO-34 synthesized by conventional method [18–20] at 200°C , using other precursors or structure directing agents and requiring autoclaved times between 48–120 hours, although always lower than the commercial material, SAPO-34c. A higher crystallinity in SAPO-34s compared with SAPO-34h can be confirmed, using the same procedure and reducing up to 4 hours the autoclaved time. The crystallization is a kinetic effect that is favored by the use of ultrasound due to the increase in the contact between the particles and the reduction of the induction period corresponding to the nucleation. The same effect has been recently described by *F. Marzpour Shalmani et al.* [21] that reported kinetic data about the enhancement of sonochemically assisted synthesis with temperature modification.

The incorporation of 2wt% of copper, concentration that is in the range used by other authors in the synthesis of these materials by impregnation or ion exchange methods for SCR application, was carried out in one step. The real amount of copper checked by XRF was 2.39 wt%. The chabazite structure was maintained, but the presence of copper caused a reduction in the degree of crystallization. *R. Martínez-Franco et al.* [10,22] indicated that the incorporation of copper in

International Journal of Innovative Research in Science, Engineering and Technology

(An ISO 3297: 2007 Certified Organization)

Vol. 5, Issue 4, April 2016

one step using unassisted conventional methods strongly depends on the gel composition but, in any case, more than 7 days are necessary to obtain a non-amorphous material. On the other side, *F. Gao et al.* [23] synthesized Cu-SAPO-34 by one-pot synthesis and solid state ion exchange and have reported that the one step process allows the incorporation of higher amounts of Cu^{2+} species to the structure, instead of CuO clusters. For the Cu-SAPO-34s, no diffraction peaks at 35.4° and 38.0° attributable to CuO were found, suggesting that copper is then well dispersed.

Rietveld refinement of the samples was carried out, obtaining the unit cell parameters a, b, and c, and the volume, which is displayed in Table 1. The SAPO-34h catalyst has a slightly lower unit cell volume than the commercial material. However, the use of ultrasound does not cause net changes in the unit cell volume. Cu-SAPO-34s material exhibited these cell unit parameters: $a = b = 13.713 \text{ \AA}$, $c = 14.915 \text{ \AA}$ and unit cell volume = 2429 \AA^3 ; similar to those estimated by *A. Turrina et al.* [24] for the Cu-SAPO-34 synthesized with another gel composition ($a = b = 13.7583 \text{ \AA}$, $c = 14.9324 \text{ \AA}$ and volume = 2448 \AA^3). The incorporation of copper caused a decrease in crystallinity associated with an increase in the unit cell volume that represents the 2.37% of SAPO-34s, suggesting that copper could be located inside the structure and causing a 3D volume expansion in consonance with the increase of $a = b$ and c distance values detected while the angles are constant, $\alpha = \beta = 90^\circ$ and $\gamma = 120^\circ$.

Table 1 Unit cell volume, surface area and pore volume of the samples

	V* (\AA^3)	Surface area ($\text{m}^2 \cdot \text{g}^{-1}$)			Pore volume ($\text{cm}^3 \cdot \text{g}^{-1}$)	
		S_μ	S_{ext}	S_{BET}	$V_{\mu\text{pore}}$	V_{total}
SAPO-34c	2389	520	10	530	0.233	0.246
SAPO-34h	2369	237	267	504	0.104	0.581
SAPO-34s	2373	185	254	439	0.081	0.509
Cu-SAPO-34s	2429	18	438	456	0.004	0.627

*By Rietveld analysis

Some changes in the morphology of the homemade materials respect to the commercial and samples synthesized by other authors have been detected. In Table 1, the calculated values of specific surface area and total pore volume are shown. Superficial area value and total pore volume of $530 \text{ m}^2 \cdot \text{g}^{-1}$ and $0.25 \text{ cm}^3 \cdot \text{g}^{-1}$, respectively, obtained for the SAPO-34c are similar to those obtained with other synthesis method [18,25], mainly indicating microporosity. The hydrothermal synthesis procedure caused a modification in the porous distribution with respect to the commercial material, providing an increase in the mesoporosity, in line with those reported by other authors[26], that prepared micro and meso SAPO-34 using different surfactants. While the surface area (S_{BET}) was similar, SAPO-34h ratio between microporous surface (S_μ) and external surface (S_{ext}) was considerably lower, as well as the ratio between micropore volume and total pore volume, whose value changed from 0.95 to 0.17, indicating a higher mesopore volume. SAPO-34s displayed values close to the SAPO-34h data, maintaining the mesoporous structure: $S_\mu/S_{\text{BET}}=0.42$ and 0.47 for SAPO-34s and SAPO-34h, respectively, and $V_\mu/V_t=0.16$. This fact is of great relevance because it indicates that modifying the route synthesis, a material with the same structure but a bi-modal pore distribution can be obtained and the process is not affected by the use of ultrasound. The incorporation of copper to the formulation, despite drastically decreasing the micropore area, contemporaneously, increases the external surface area. So, copper must be located inside the cavities, occupying without blocking the micropores of the structure.

The different TEM images and ED pattern (Fig. 2) show practically cubic structure crystals, with a greater size for the traditional hydrothermal method synthesized material. SAPO-34h ED pattern presents a structure that might be due to a low order degree. Nevertheless, the use of ultrasound in the synthesis produces an increase in the crystallinity, which is tested by the most intense rings. This observation is in accordance with XRD diffractograms and Rietveld analysis.

a

b

c

International Journal of Innovative Research in Science, Engineering and Technology

(An ISO 3297: 2007 Certified Organization)

Vol. 5, Issue 4, April 2016

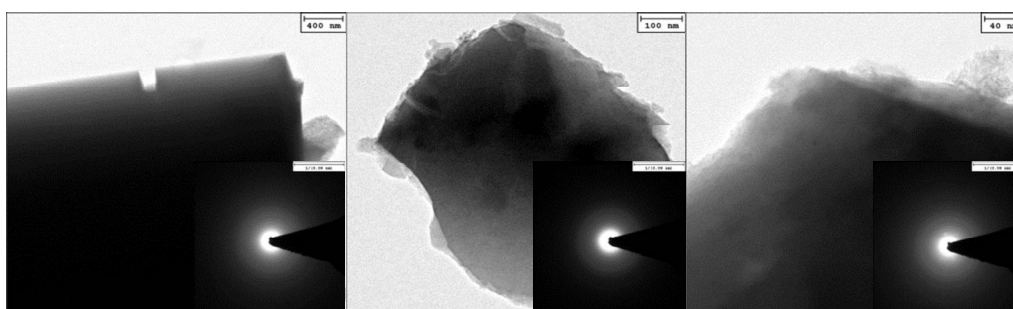


Fig. 2TEM images (insert ED pattern) of (a) SAPO-34h(b) SAPO-34s and (c)Cu-SAPO-34s

Dark spots, mainly attributed to CuO as other authors [6] have detected when ion exchange and wetness impregnation synthesis methods are used, were not observed in the Cu-SAPO-34s TEM images. Copper was detected by microanalysis. It is possible to observe crystals of 0.3nm of distance in the ED pattern, which corresponds to copper lattice constant. To check the copper presence in the sample, EDX mapping was performed and the obtained images are represented in Fig. 3, where all the elements presented in a particle were analyzed.

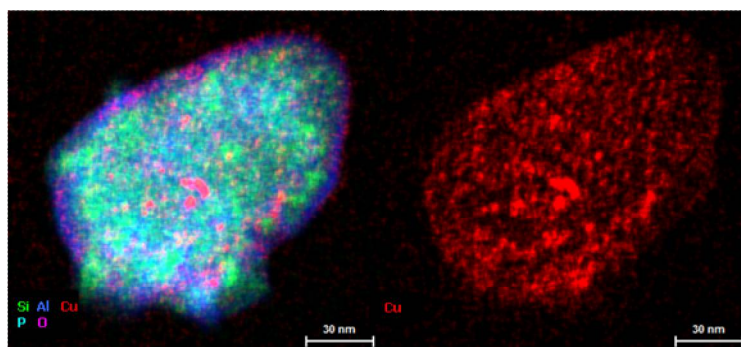


Fig. 3EDX mapping image of Cu-SAPO-34s with the representation of all element (right figure) or only copper (left part of the image)

There is a homogeneous distribution of silicon, aluminum and phosphorus and the weight percentage of each element is in consonance with gel composition and the X-ray fluorescence data. In particular, the detection of copper shows an extremely high dispersion of this element along the whole particle and clusters are not evidenced. The SEM images for the synthesized SAPO-34 materials are shown in Fig.4.

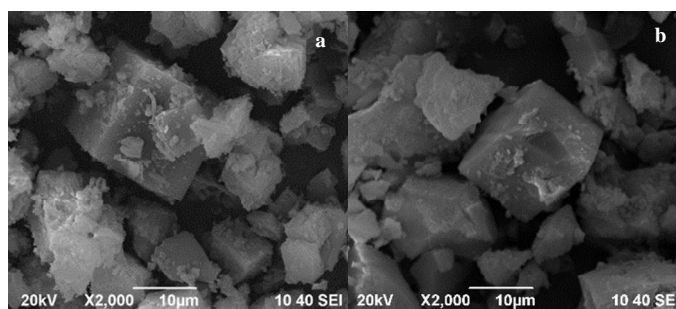


Fig. 4SEM images of (a) SAPO-34h and (b) SAPO-34s

Materials not containing copper revealed cubic crystals with sizes between 6 and 10 µm, which is in consonance with the literature [10,23,27], where similar particles are observed but slight differences were detected depending on the

International Journal of Innovative Research in Science, Engineering and Technology

(An ISO 3297: 2007 Certified Organization)

Vol. 5, Issue 4, April 2016

synthesis method and the autoclaved temperature. In addition, some part of the precursor gel was not removed in the washing process, so remains of aluminum are observed in synthesized catalysts. It can be seen that the ultrasonic assisted synthesized sample shows higher crystallized cubes, in agreement with the other characterization techniques.

The UV-Visible spectra of the ultrasound assisted synthesized samples are shown in Fig.5. For the SAPO-34s, there is lack of absorption in the whole spectra, a weak band around 255 nm is only observed and associated with the charge transfer (CT) band of the zeolite ($O^{2-} \rightarrow Al^{3+}$) as it has been reported by other authors [28] for other aluminophosphates.

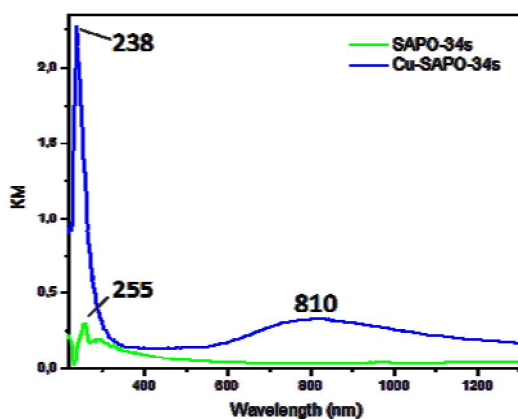


Fig. 5 UV-Vis DR spectra of SAPO-34s and Cu-SAPO-34s

In the case of Cu-SAPO-34s, an intense band centered at 238 nm and a broad band extended around a maximum localized at 810 nm are registered. The most energetic signal is attributed to $O^{2-} \rightarrow Cu^{2+}$ ligand to metal charge transfer transition of isolated Cu^{2+} species as *M. Turco et al.* [29] previously reported in the study of a hydrotalcite with copper and the second one is assigned to electron d-d transitions of Cu^{2+} ions in distorted octahedral symmetry. There are no bands detected at 355 or 456 nm, which are associated with the CT bands of O-Cu-O and Cu-O-Cu complexes, respectively, as other authors have observed [30,31] when Cu/SAPO-34 is obtained by ion exchange or precipitation methods, which confirms the absence of these types of species with the one-pot ultrasound assisted synthesis. Therefore, it has been confirmed by different techniques that CuO segregates or clusters are not detected and hence, copper is highly dispersed and isolated Cu^{2+} species are observed. So, in contrast to Cu-SAPO-34 post-synthesis incorporation methods, such as impregnation or ion exchange, the current one-pot synthesis process produces a material with copper located inside the structure and uniformly distributed as Cu^{2+} species.

As is well-known and previously reported [32,33], both the copper sites and the acidity are the main factors for the NH_3 -SCR reaction on Cu-CHA catalysts. In fact, it is recognized that Brönsted acid sites are thought to be the active sites for SCR process. So, to study the interaction between catalysts and the feeding N-containing gases of the SCR process, FTIR spectra of self-supporting catalysts disks were recorded. The subtraction of the activated material spectrum to NH_3 adsorption spectra are displayed in Fig.6. The retention takes place mainly with Brönsted species formation for no Cu-containing materials, with a maximum signal at 1453 cm^{-1} and a shoulder at 1400 cm^{-1} associated with different P, Al and Si species, as other authors have observed [34] for commercial materials. A weak signal at 1623 cm^{-1} was observed and related to residual ammonia coordinated over Lewis Acid Sites (LAS). After evacuation at 300°C all signals almost disappeared for Cu-free materials due to the weak interaction of thermally stable species.

International Journal of Innovative Research in Science, Engineering and Technology

(An ISO 3297: 2007 Certified Organization)

Vol. 5, Issue 4, April 2016

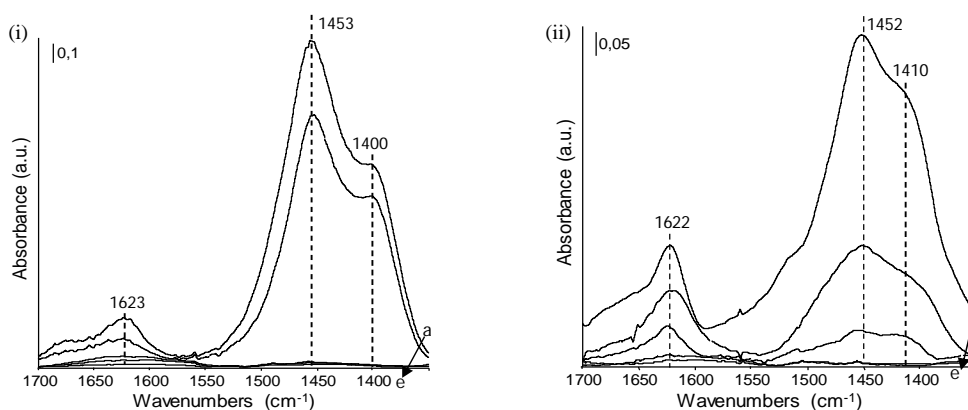


Fig. 6 FTIR spectra of 10 torr of NH_3 adsorbed on (i) SAPO-34s and (ii) Cu-SAPO-34s from (a) 100°C to (e) 500°C

For Cu-SAPO-34s, after evacuation at 100°C, modes centered at 1452, 1410 (sh) cm^{-1} and a more intense signal at 1622 cm^{-1} were registered (Fig. 6 (ii)). The modes associated with Brönsted Acid Sites (BAS) remained up to 300°C, as well as the additional LAS provided by the presence of copper.

Additionally, isothermal NH_3 adsorption runs were performed in a fix bed reactor (pulse of 1000ppm of NH_3 in He, 20 min/35 min of He purge) to calculate the net ammonia adsorption capacity at different temperatures indicating that for SAPO-34s in the low temperature of the SCR range (200°C) was around $70\mu\text{mol}\cdot\text{g}^{-1}$ while for Cu-SAPO-34s, $84\mu\text{mol}$ of adsorbed ammonia per gram of catalyst were obtained, which represents an increase of 20wt% over the total acidity of the materials; as a result, Cu-SAPO-34s can be used as an effective NH_3 -trap.

NO adsorption was studied in the same conditions as ammonia probe molecule adsorption. In Fig.7(i), NO adsorption onto SAPO-34s showed bands between 1500-1700 cm^{-1} and can be assigned to different nitrates and nitrites species. Despite of the complexity to identify these peaks due to the very similar vibrations of the different nitrate species, for this catalyst, a band around 1630 cm^{-1} associated with the presence of bridged nitrate groups was observed and a less intense signal at 1590 cm^{-1} related to bidentate nitrate groups was detected. In addition, a broad and weak band around 1480 cm^{-1} corresponding to nitrites was also evidenced. In absence of oxygen, the accumulation of NO over the catalyst makes the formation of these species possible, which disappear after evacuation at 300°C.

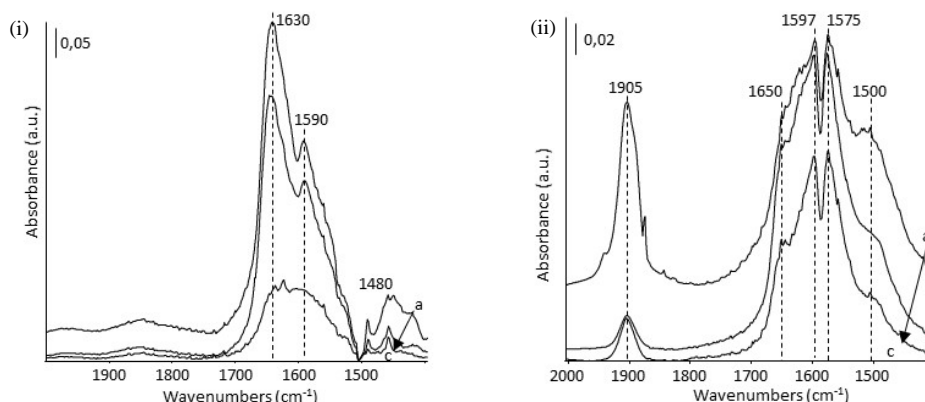


Fig. 7 FTIR spectra of 10 torr of NO adsorbed on (i) SAPO-34s and (ii) Cu-SAPO-34s from (a) 100°C to (c) 300°C

On the contrary, for Cu-SAPO-34s the profile is quite different. Below 1800 cm^{-1} , intense modes at 1650, 1597 and 1575 cm^{-1} compared. An additional strong signal was observed at 1905 cm^{-1} , characteristic of isolated Cu^{2+} ions in

International Journal of Innovative Research in Science, Engineering and Technology

(An ISO 3297: 2007 Certified Organization)

Vol. 5, Issue 4, April 2016

square pyramidal configuration. The chemical environment modified by the copper incorporation and localization causes several effects: a) splitting of the signal at 1590cm^{-1} into two modes at 1597 and 1575cm^{-1} associated with bidentate nitrate groups over different species, b) shifting of the band at 1630 to 1650cm^{-1} , indicating the presence of bridged nitrate groups more strongly anchored to the catalyst and c) the shoulder below 1500cm^{-1} related to nitrite groups is modified to higher energy. At 100°C it is possible to detect a band at 1940cm^{-1} , assigned to Cu^{2+} sites and a shoulder around 1890cm^{-1} related to NO interacting with the OH group of $[\text{Cu-OH}]^+$ sites (modes at 1898 - 1880cm^{-1}). It should be noticed that other species such as Cu^+ mononitrosyl complex $[\text{Cu}^+(\text{NO})]$ (band at 1755cm^{-1}) or NO adsorbed on another type of Cu^{2+} sites, such as Cu_xO_y clusters (band at 1897cm^{-1}) were not detected. When the sample is heated at 200°C , the main signals remained even at temperatures above 300°C . It is well-known that isolated Cu^{2+} species on Cu-SAPO-34 are the active sites for the NH_3 -SCR reaction [13,16,32] and are very stable when harsh hydrothermal treatments are performed with similar catalysts as *R. Martínez-Franco et al.* [22] have reported. Additional experiments were carried out by steaming the Cu-SAPO-34s with water at 750°C for several hours and there was no apparently modification of the chabazite structure, checked by XRD.

At this point, the presence of Cu^{2+} species, active in NO adsorption, has been confirmed, together with Brönsted and Lewis acidic sites. In atmosphere of NO, Cu-SAPO-34s allows the retention of nitrate species and mononitrosyl $[\text{Cu}^+(\text{NO})]$ species; nitrates are mainly related to the interaction with the support, although can be energetically modified by the presence of copper and mononitrosyl species are the most likely intermediates in the SCR mechanism. To study the species involved into the SCR mechanism, the co-adsorption of NH_3 , NO and O_2 was carried out. In Fig.8 (a), the spectrum after ammonia adsorption at 300°C is represented. Modes around 1621 and 1452cm^{-1} are observed that are associated with Lewis and Brönsted acid sites, respectively, and are in agreement with NH_3 adsorption spectra explained above. At this temperature, the amount of Lewis acid sites more stable and related to the presence of copper increased. In all spectra, a signal at 1350cm^{-1} can be observed and it corresponds to the potassium nitrate formed in the cell KBr window.

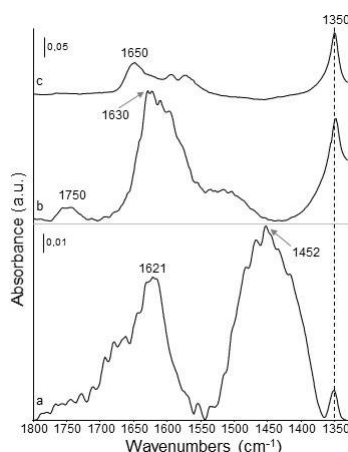


Fig. 8FTIR co-adsorption spectra over Cu-SAPO-34s at 300°C after: (a) NH_3 adsorption and evacuation, (b) 15 min in $\text{NO} + \text{O}_2$ atmosphere and (c) the evacuation of all the gas phase

After the introduction of NO and oxygen, a prompt nitrogen formation was monitored by MS and a broad band between 1500 and 1700cm^{-1} was observed in the spectrum (Fig. 8(b)). The SCR reaction with the retained ammonia is responsible for the nitrogen production, and the excess of NO and O_2 causes the accumulation of different nitrate species. A less intense band around 1750cm^{-1} was also detected and can be related to the interaction of NO with Cu^+ or NO dimers. In any case, all these species act as spectators of the reaction. At the end of the process, only a slow amount of nitrates remained over the surface, indicating the complete removal of the adsorbed ammonia and the practically total regeneration of the catalyst.

International Journal of Innovative Research in Science, Engineering and Technology

(An ISO 3297: 2007 Certified Organization)

Vol. 5, Issue 4, April 2016

Tests performed in SCR atmosphere (750 ppm NO+ 750 ppm NH₃ + 3%O₂) were carried out and NO and NH₃ conversions and N₂ selectivity at different temperatures were calculated when stationary conditions were achieved. For SAPO-34s, no NH₃ and NO conversion or nitrogen production were detected in the SCR temperature range. Nevertheless, nitrates formation and ammonia adsorption were observed by IR of probe molecules. As a result, SAPO-34 material is effective as NH₃ traps but is not useful for the SCR process. The SCR activity for Cu-SAPO-34s (Fig.9), showed high NO conversion values in the whole SCR range, similar to those obtained by other authors who, despite preparing the materials by post-synthesis methods, have observed the same behavior [20,35]. NH₃ conversion increased with the temperature and was slightly lower than NO conversion at low temperatures.

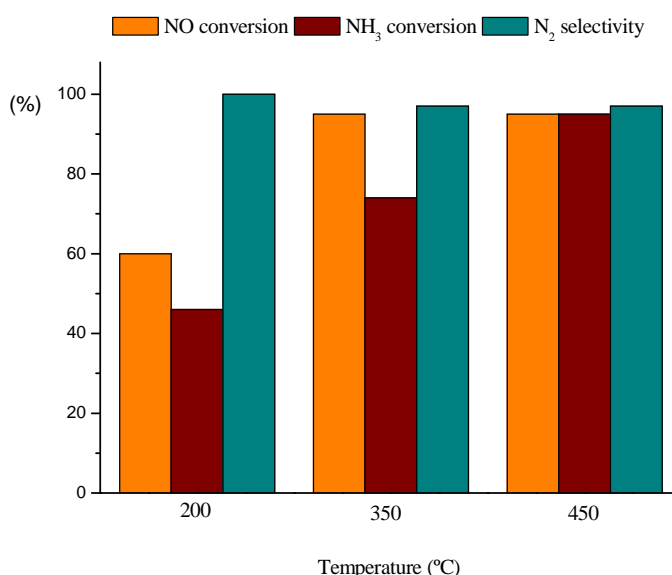


Fig. 9Cu-SAPO-34s SCR activity values (NO and NH₃ conversion and N₂ selectivity) in the range of temperature

At the lowest temperature value for the SCR, this fact could be explained considering that the amount of adsorbed nitrates is higher than the ammonia retention, so this catalyst structure favors the NO conversion due to the reaction with ammonia in addition to the nitrate formation. At 350°C, the conversions values are higher but still different, due to the coupling of the standard SCR reaction with the nitrates decomposition that takes place, close to this temperature, with nitrogen formation. At high temperature only the standard SCR reaction occurs, in consonance with the stoichiometric consumption of the reagents. It should be pointed out that the selectivity to N₂ is complete in the whole SCR range, with negligible detection of other undesired products, such as ammonia or N₂O.

So, it can be confirmed that the incorporation of copper in the SAPO-34 structure is necessary to have active species for the SCR process and, also, the preparation route explained in this work makes the location of copper as Cu²⁺ isolated mainly species possible, which are the active sites in the reaction.

IV. CONCLUSIONS

The methodology proposed in this work allows the synthesis of a material with chabazite-like structure and 2 wt% of copper inside the framework. Ultrasound assisted synthesis of SAPO-34 considerably reduces the time of synthesis and provides materials with higher crystallinity compared to traditionally synthesized samples. The 3D volume expansion obtained by Rietveld analysis confirmed that copper is located inside the structure. The SCR activity of this

International Journal of Innovative Research in Science, Engineering and Technology

(An ISO 3297: 2007 Certified Organization)

Vol. 5, Issue 4, April 2016

material was tested, being Brönsted acid sites and $\text{Cu}^{2+}(\text{NO})$ species detected, and providing complete selectivity to nitrogen in the whole SCR temperature range.

ACKNOWLEDGEMENTS

MCR acknowledges the Spanish Ministry of Education, Culture and Sport for a FPU grant (FPU12/03826). The authors wish to thank Albemarle Corporation the supply of the materials. Authors want to thank the financial support of CTQ 2013-47853R Project.

REFERENCES

- [1] Omidvarborna, H., Kumar, A., and Kim, D.-S., "NO_x emissions from low-temperature combustion of biodiesel made of various feedstocks and blends", *Fuel Processing Technology*, Vol.140, pp.113–118, 2015.
- [2] Lanjekar, R.D., and Deshmukh, D., "A review of the effect of the composition of biodiesel on NO_x emission, oxidative stability and cold flow properties", *Renewable and Sustainable Energy Reviews*, Vol.54, pp.1401–1411, 2016.
- [3] Hou, X., Schmiege, S.J., Li, W., and Epling, W.S., "NH₃ pulsing adsorption and SCR reactions over a Cu-CHA SCR catalyst", *Catalysis Today*, Vol.197, pp.9–17, 2012.
- [4] Ruggeri, M.P., Nova, I., Tronconi, E., Pihl, J.A., Toops, T.J., and Partridge, W.P., "In-situ DRIFTS measurements for the mechanistic study of NO oxidation over a commercial Cu-CHA catalyst", *Applied Catalysis B: Environmental*, Vol.166–167, pp.181–192, 2015.
- [5] Pieta, I.S., García-Diéguez, M., Herrera, C., Larrubia, M.A., and Alemany, L.J., "In situ DRIFT-TRM study of simultaneous NO_x and soot removal over Pt-Ba and Pt-K NSR catalysts", *Journal of Catalysis*, Vol.270, pp.256–267, 2010.
- [6] Pereda-Ayo, B., De La Torre, U., Illán-Gómez, M.J., Bueno-López, A., and González-Velasco, J.R., "Role of the different copper species on the activity of Cu/zeolite catalysts for SCR of NO_x with NH₃", *Applied Catalysis B: Environmental*, Vol.147, pp.420–428, 2014.
- [7] De La Torre, U., Pereda-Ayo, B., and González-Velasco, J.R., "Cu-zeolite NH₃-SCR catalysts for NO_x removal in the combined NSR-SCR technology", *Chemical Engineering Journal*, Vol.207–208, pp.10–17, 2012.
- [8] Lindholm, A., Sjövall, H., and Olsson, L., "Reduction of NO_x over a combined NSR and SCR system", *Applied Catalysis B: Environmental*, Vol.98, pp.112–121, 2010.
- [9] Colombo, M., Nova, I., and Tronconi, E., "Detailed kinetic modeling of the NH₃-NO/NO₂ SCR reactions over a commercial Cu-zeolite catalyst for Diesel exhausts after treatment", *Catalysis Today*, Vol.197, pp.243–255, 2012.
- [10] Martínez-Franco, R., Moliner, M., Franch, C., Kustov, A., and Corma, A., "Rational direct synthesis methodology of very active and hydrothermally stable Cu-SAPO-34 molecular sieves for the SCR of NO_x", *Applied Catalysis B: Environmental*, Vol.127, pp.273–280, 2012.
- [11] Kim, Y.J., Lee, J.K., Min, K.M., Hong, S.B., Nam, I.-S., and Cho, B.K., "Hydrothermal stability of CuSSZ13 for reducing NO_x by NH₃", *Journal of Catalysis*, Vol.311, pp.447–457, 2014.
- [12] Ma, L., Cheng, Y., Cavataio, G., McCabe, R.W., Fu, L., and Li, J., "In situ DRIFTS and temperature-programmed technology study on NH₃-SCR of NO_x over Cu-SSZ-13 and Cu-SAPO-34 catalysts", *Applied Catalysis B: Environmental*, Vol.156–157, pp.428–437, 2014.
- [13] Wang, D., Jangjou, Y., Liu, Y., Sharma, M.K., Luo, J., Li, J., Kamasamudram, K., and Epling, W.S., "A comparison of hydrothermal aging effects on NH₃-SCR of NO_x over Cu-SSZ-13 and Cu-SAPO-34 catalysts", *Applied Catalysis B: Environmental*, Vol.165, pp.438–445, 2015.
- [14] Beretta, A., Tronconi, E., Alemany, L.J., Svachula, J., and Forzatti, P., "Effect of morphology of honeycomb SCR catalysts on the reduction of NO_x and the oxidation of SO₂", *New Developments in Selective Oxidation II*, pp.869–876, 1994.
- [15] Colombo, M., Nova, I., and Tronconi, E., "A comparative study of the NH₃-SCR reactions over a Cu-zeolite and a Fe-zeolite catalyst", *Catalysis Today*, Vol.151, pp.223–230, 2010.
- [16] Deka, U., Lezcano-Gonzalez, I., Warrender, S.J., Picone, A.L., Wright, P.A., Weckhuysen, B.M., and Beale, A.M., "Changing active sites in Cu-CHA catalysts: deNO_x selectivity as a function of the preparation method", *Microporous and Mesoporous Materials*, Vol.166, pp.144–152, 2013.
- [17] Picone, A.L., Warrender, S.J., Slawin, A.M.Z., Dawson, D.M., Ashbrook, S.E., Wright, P.A., Thompson, S.P., Gaberova, L., Llewellyn, P.L., Moulin, B., Vimont, A., Daturi, M., Park, M.B., Sung, S.K., Nam, I.-S., and Hong, S.B., "A co-templating route to the synthesis of Cu SAPO STA-7, giving an active catalyst for the selective catalytic reduction of NO", *Microporous and Mesoporous Materials*, Vol.146, pp.36–47, 2011.
- [18] Álvaro-Muñoz, T., Márquez-Álvarez, C., and Sastre, E., "Use of different templates on SAPO-34 synthesis: Effect on the acidity and catalytic activity in the MTO reaction", *Catalysis Today*, Vol.179, pp.27–34, 2012.
- [19] Cui, Y., Zhang, Q., He, J., Wang, Y., and Wei, F., "Pore-structure-mediated hierarchical SAPO-34: Facile synthesis, tunable nanostructure, and catalysis applications for the conversion of dimethyl ether into olefins", *Particuology*, Vol.11, pp.468–474, 2013.
- [20] Petitto, C., and Delahay, G., "Selective catalytic reduction of NO_x by NH₃ on Cu-SAPO-34 catalysts: Influence of silicon content on the activity of calcined and hydrotreated samples", *Chemical Engineering Journal*, Vol.264, pp.404–410, 2015.
- [21] Marzpour Shalmani, F., Halladj, R., and Askari, S., "An investigation of the crystallization kinetics of zeotype SAPO-34 crystals synthesized by hydrothermal and sonochemical methods", *Ultrasonics Sonochemistry*, Vol.29, pp.354–362, 2016.
- [22] Martínez-Franco, R., Moliner, M., Concepcion, P., Thøgersen, J.R., and Corma, A., "Synthesis, characterization and reactivity of high hydrothermally stable Cu-SAPO-34 materials prepared by "one-pot" processes", *Journal of Catalysis*, Vol.314, pp.73–82, 2014.
- [23] Gao, F., Walter, E.D., Washton, N.M., Szanyi, J., and Peden, C.H.F., "Synthesis and evaluation of Cu/SAPO-34 catalysts for NH₃-SCR₂: Solid-state ion exchange and one-pot synthesis", *Applied Catalysis B: Environmental*, Vol.162, pp.501–514, 2015.
- [24] Turrina, A., Eschenroeder, E.C.V., Bode, B.E., Collier, J.E., Apperley, D.C., Cox, P.A., Casci, J.L., and Wright, P.A., "Understanding the structure directing action of copper-polyamine complexes in the direct synthesis of Cu-SAPO-34 and Cu-SAPO-18 catalysts for the selective catalytic reduction of NO with NH₃", *Microporous and Mesoporous Materials*, Vol.215, pp.154–167, 2015.

International Journal of Innovative Research in Science, Engineering and Technology

(An ISO 3297: 2007 Certified Organization)

Vol. 5, Issue 4, April 2016

- [25] Liu, G., Tian, P., Li, J., Zhang, D., Zhou, F., and Liu, Z., "Synthesis, characterization and catalytic properties of SAPO-34 synthesized using diethylamine as a template", *Microporous and Mesoporous Materials*, Vol.111, pp.143–149, 2008.
- [26] Singh, A.K., Yadav, R., and Sakthivel, A., "Synthesis, characterization, and catalytic application of mesoporous SAPO-34 (MESO-SAPO-34) molecular sieves", *Microporous and Mesoporous Materials*, Vol.181, pp.166–174, 2013.
- [27] Askari, S., Sedighi, Z., and Halladj, R., "Rapid synthesis of SAPO-34 nanocatalyst by dry gel conversion method templated with morpholine: Investigating the effects of experimental parameters", *Microporous and Mesoporous Materials*, Vol.197, pp.229–236, 2014.
- [28] Dang, T.T.H., Zubowa, H.-L., Bentrup, U., Richter, M., and Martin, A., "Microwave-assisted synthesis and characterization of Cu-containing AlPO₄-5 and SAPO-5", *Microporous and Mesoporous Materials*, Vol.123, pp.209–220, 2009.
- [29] Turco, M., Bagnasco, G., Costantino, U., Marmottini, F., Montanari, T., Ramis, G., and Busca, G., "Production of hydrogen from oxidative steam reforming of methanol. I. Preparation and characterization of Cu/ZnO/Al₂O₃ catalysts from a hydrotalcite-like LDH precursor", *Journal of Catalysis*, Vol.228, pp.43–55, 2004.
- [30] Leistner, K., and Olsson, L., "Deactivation of Cu/SAPO-34 during low-temperature NH₃-SCR", *Applied Catalysis B: Environmental*, Vol.165, pp.192–199, 2015.
- [31] Wang, L., Gaudet, J.R., Li, W., and Weng, D., "Migration of Cu species in Cu/SAPO-34 during hydrothermal aging", *Journal of Catalysis*, Vol.306, pp.68–77, 2013.
- [32] Ma, L., Cheng, Y., Cavataio, G., McCabe, R.W., Fu, L., and Li, J., "Characterization of commercial Cu-SSZ-13 and Cu-SAPO-34 catalysts with hydrothermal treatment for NH₃-SCR of NO_x in diesel exhaust", *Chemical Engineering Journal*, Vol.225, pp.323–330, 2013.
- [33] Bates, S.A., Delgass, W.N., Ribeiro, F.H., Miller, J.T., and Gounder, R., "Methods for NH₃ titration of Brønsted acid sites in Cu-zeolites that catalyze the selective catalytic reduction of NO_x with NH₃", *Journal of Catalysis*, Vol.312, pp.26–36, 2014.
- [34] Wang, L., Li, W., Qi, G., and Weng, D., "Location and nature of Cu species in Cu/SAPO-34 for selective catalytic reduction of NO with NH₃", *Journal of Catalysis*, Vol.289, pp.21–29, 2012.
- [35] Panahi, P.N., Niaei, A., Salari, D., Mousavi, S.M., and Delahay, G., "Ultrasound-assisted preparation of Cu-SAPO-34 nanocatalyst for selective catalytic reduction of NO by NH₃", *Journal of Environmental Sciences*, Vol.35, pp.135–143, 2015.